7-12-2013

Direct Imaging of Optical Diffraction in Photoemission Electron Microscopy

Robert Campbell Word
Portland State University

Joseph Fitzgerald
Portland State University

Rolf Könenkamp
Portland State University, rkoe@pdx.edu

Citation Details

Word, Robert C., J. P. S. Fitzgerald, and Rolf Konenkamp. "Direct imaging of optical diffraction in photoemission electron microscopy." Applied Physics Letters 103.2 (2013): 021118-021118.

AIP | Applied Physics Letters

Direct imaging of optical diffraction in photoemission electron microscopy

Robert C. Word, J. P. S. Fitzgerald, and Rolf Könenkamp

Citation: Appl. Phys. Lett. **103**, 021118 (2013); doi: 10.1063/1.4813550
View online: http://dx.doi.org/10.1063/1.4813550
View Table of Contents: http://apl.aip.org/resource/1/APPLAB/v103/i2
Published by the AIP Publishing LLC.

Direct imaging of optical diffraction in photoemission electron microscopy

Robert C. Word, J. P. S. Fitzgerald, and Rolf Könenkamp[a)]
Physics Department, Portland State University, 1719 SW 10th Avenue, Portland, Oregon 97201, USA

(Received 24 May 2013; accepted 23 June 2013; published online 12 July 2013)

We report the visualization of optical diffraction at the boundaries of semiconductor and metal nanostructures in non-linear photoemission electron microscopy. We observe light diffracting into photonic and plasmonic modes of planar samples, and into photonic vacuum modes above sample surfaces. In either case, the electron photoemission rate from the sample material is spatially modulated resulting in photoemission images with information on the electric field distribution at the sample/vacuum interface. The resolution in these images is typically ~30 nm, i.e., significantly below the wavelengths of the exciting light. Optical phase shifts and absorption losses for the diffracted modes can be determined. © *2013 AIP Publishing LLC*. [http://dx.doi.org/10.1063/1.4813550]

The nanoscale observation of optical phenomena at semiconductor and metal surfaces is receiving increased interest, as optical information processing now approaches frequencies in the visible spectral region and device sizes have moved into the submicron range. Scanning probe techniques have been used to characterize phenomena in near-field optics.[1,2] Photoemission electron microscopy (PEEM) has recently been employed for the visualization of plasmonic effects,[3–6] and earlier work has demonstrated its sensitivity to local variations of the electric field near protruding features at surfaces.[7] Here we show with three different examples that PEEM can directly and quantitatively visualize diffraction phenomena at solid surfaces. We show the emergence of photonic modes in the vicinity of transparent and absorbing semiconductors and the emergence of plasmonic modes at metal surfaces. A quantitative evaluation of the obtained images allows a distinction between modes that propagate inside the samples with propagation parameters given by the sample dielectric constant, and modes propagating above the sample surface in vacuum and subject to the vacuum dielectric properties.

PEEM uses the photoelectric effect for the photoemission of electrons from surfaces. In our work, the excitation photon energies are chosen such that the electron exit energies are below ~1 eV. These photoelectrons are subsequently accelerated and enter an electron microscope column where spatial images of the emitting surface are generated. PEEM thus combines photon-based probing with the high-resolution capabilities of electron imaging. The electron excitation energies necessary for photoemission have to be larger than the work-function energy, which in the present cases is between 4 and 6 eV. This energy can be provided in single-photon excitations with ultraviolet light or, alternatively, in multi-photon excitations with visible or even infrared light.[9,10] Multi-photon excitation thus allows photoemission microscopy in the visible and fiber-optical wavelength region. It has the additional advantage to provide enhanced image contrast due to the non-linearity of the excitation process.[11] As the efficiency of multi-photon processes increases with light intensity, pulsed laser excitation is typically used in this operation mode.

The experiments were performed in an aberration-corrected photoemission electron microscope with an optimum resolution of 5 nm.[12] In the current experiments, the resolution is approximately 30 nm. We use a frequency doubled pulsed Ti:sapphire providing 80 fs pulses at a wavelength of 410 nm, repetition rate of 100 MHz, and pulse energies of 5 nJ, or a cw frequency-doubled Ar^+-ion laser at 244 nm. Indium-tin-oxide (ITO) samples were acquired from SPI Inc. and had a conductivity of 10 Ω/sq. The structured Si wafer, a calibration standard, was obtained from Ted Pella, Inc., and gold nano-platelets were prepared by solution-based chemical growth following a recipe given in Refs. 13 and 14.

The imaging of the diffraction utilizes the interference of the diffracted light with the un-diffracted incident light beam in a geometry as shown in Figure 1. The resulting interference pattern is stationary in space and can be imaged in PEEM, as the light distribution near the surface affects the photoemission rate. A quantitative evaluation is possible when the optical parameters of the sample and the geometry are known. We take as a first example the case of a transparent indium-tin-oxide film deposited on glass substrate.[15] The ITO is provided with a horizontal groove oriented perpendicularly to the incidence direction and a slightly depressed center area, both milled in a focused ion beam. At the groove, the excitation laser light is coupled into the film by diffraction. The ITO then acts as a waveguide for the diffracted light. Here we only discuss the slightly thinner center area of the ITO film. Applying waveguide theory, one can calculate the allowed guided modes and their associated effective refractive indices.[15–18] With this information, the observed interference pattern is completely determined. For a quantitative analysis, we describe the incident and diffracted waves as

$$\begin{aligned} E_{inc}(y,t) &= A\exp(i(ky\sin\theta - \omega t)),\\ E_j(y,t) &= B_j\exp(i(kyN_j - \omega t)), \end{aligned} \tag{1}$$

where A and B are the incident and diffracted wave amplitudes, E is the electric field amplitude, k is the wave number of the incident light, θ is the angle of incidence with respect to the sample normal, y is the propagation direction in the sample plane, and N is the effective refractive index for the

[a)]Author to whom correspondence should be addressed. Electronic mail: rkoe@pdx.edu

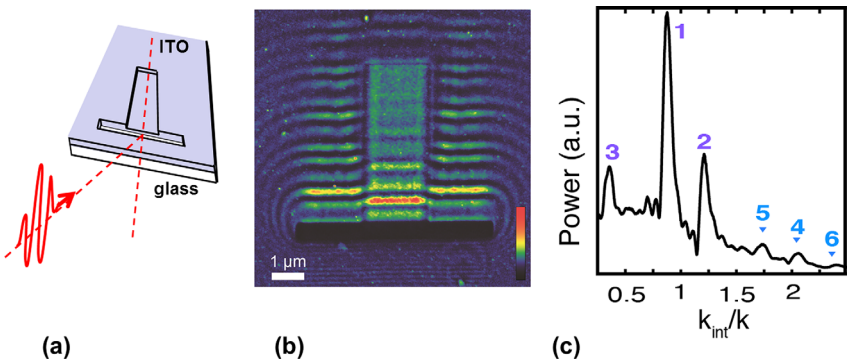

FIG. 1. Schematic of the illumination and diffraction geometry at the groove in a planar ITO-film. (b) Interference pattern observed in PEEM for TM polarization of the excitation light. (c) Spatial Fourier spectrum of the experimental interference pattern along the propagation direction showing well discerned peaks for two guided modes (1 and 2), the difference frequency mode (3), and their higher order modes (4–6) caused by the non-linearity in the 2-photon excitation.

diffracted wave. The index j relates to the various possible modes of the guided wave. Superimposing E_{inc} and E_j, taking the squared absolute value, and integrating over time produces the observed stationary interference pattern. In single-photon excitation, the photoemission rate would be proportional to the interference pattern intensity; in the case of two-photon excitation as used here the emission rate is proportional to the squared intensity. In the current case we find two guided modes, and in the limit of cw illumination, the photoemission yield is given by

$$I_{PE} \propto (|A\exp(iky\sin\theta) + B_1\exp(ikyN_1) + B_2\exp(ikyN_2)|^2)^2. \quad (2)$$

When the diffracted modes have small amplitudes, i.e., $B_j \ll A$, the modulation amplitude in the interference pattern is proportional to the electric field amplitude of the diffracted waves,

$$I_{PE} \propto A^4 + 4A^3(B_1\cos(ky(N_1 - \sin\theta)) + B_2\cos(ky(N_2 - \sin\theta))) + O(B^2), \quad (3)$$

as discussed in more detail in Ref. 15. Fitting the model to the experimental data allows a determination of the coupling coefficients, B_j/A, for the diffraction. Fig. 1(c) shows the spatial Fourier transform of the interference pattern. For the central region, which has a lower thickness than the surrounding, the guided modes have effective indices 1.72 and 2.04, respectively. From the peak widths, an absorption coefficient of $\alpha = 8000\,\text{cm}^{-1}$ can be derived. These values are in good agreement with the known optical properties of ITO[19] and a detailed waveguide model as discussed in more detail in Ref. 15. Additionally, the Fourier transform shows clear signatures of the difference frequency mode and higher order modes in the signals labeled 3–6. The obtained data are also of sufficient quality to determine phase shifts at the diffraction occurring at the diffraction source.

Replacing the transparent ITO film with a highly absorbing silicon wafer strongly suppresses wave propagation within the sample material, as the optical absorption coefficient at the used wavelength of 244 nm is $\alpha = 4 \times 10^6$ cm^{-1}, corresponding to an absorption length of only 3 nm. Yet a diffraction-based interference pattern is still observed in this case as shown in Figure 2. The analysis of the diffraction pattern shows that the diffracted wave propagates in a medium with refractive index $n = 1$, indicating that the photoemission image is now due to interference between a diffracted wave propagating through vacuum and the incident light. This wave is apparently part of a cylindrical wave scattered by a linear feature at the Si surface and propagating in the vacuum above the Si surface.[24] The physical mechanism to generate the photoemission image in this case is the spatially varying electric-field amplitude immediately above the samples surface. Apparently the spatially modulated field strength changes the photoemission rate. The electric field dependence of the photoemission rate has been noted in several recent experiments.[8] Fig. 2(b) shows that similar to the waveguide case in ITO, the experimental data are good enough to establish phase shifts occurring within the near-field of the diffracting edge feature as well as amplitude losses along the propagation. In the present case, we have fitted the data with an exponential decay of 470 ± 50 nm, even though a mixed algebraic decay law may be more appropriate for the cylindrical geometry.[20]

Finally in Fig. 3, we present another case of interest where the diffraction process generates a surface plasmon polariton in a planar 50 nm thick, single-crystalline gold platelet. From the well-known optical data for gold,[21,22] it can be shown that within the gold crystal photonic modes are not supported at excitation wavelengths of 410 nm, only plasmonic surface modes can propagate. An analytical treatment[23] based on an asymmetric 3-layer model[24] for the ITO/gold/vacuum sample configuration gives a consistent description in terms of surface plasmon propagation. The plasmon propagation velocity and decay length can directly

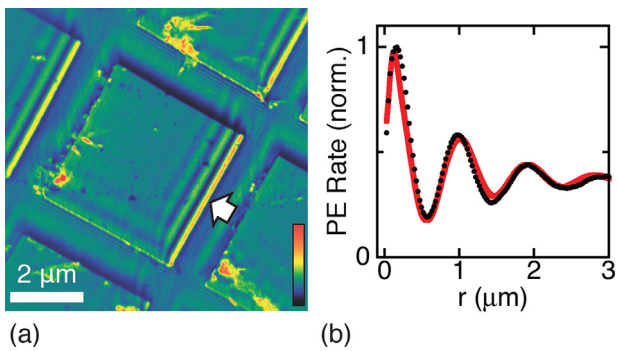

FIG. 2. Ultraviolet PEEM micrograph of diffraction at the edges of a nanostructured Si wafer. The arrow indicates the direction for the line scan. (b) Photoemission line profile in the direction of the arrow in (a). The experimental data are plotted as black dots, the calculated profile is plotted as a continuous line in red and is based on a propagation velocity $v = c$ and a decay length of $\lambda = 470$ nm.

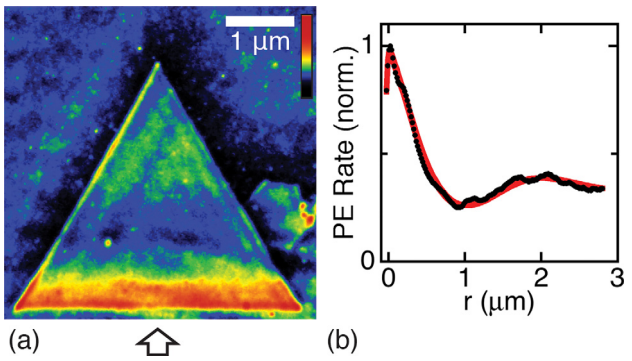

FIG. 3. (a) Interference pattern relating to surface plasmons generated in a triangular gold platelet of 50 nm thickness visualized in 2-photon photoemission electron microscopy using 410 nm pulsed light. (b) Line profile of the photoemission rate taken perpendicular to the bottom edge as indicated by the arrow in (a); black dots: experimental data, red line: fit based on optical data of Ref. 22 with a surface plasmon decay length of 380 nm.

be calculated from the optical data.[21] These data predict a plasmon propagation velocity of $v = 0.98\,c$ and a decay length $\lambda = 378$ nm. Figure 3(b) shows a line scan of the interference pattern at the bottom edge. Fitting these results with $v = 0.98\,c$ for the propagation speed and $\lambda = 380 \pm 10$ nm for the decay length gives excellent agreement with the model. Again the quality of the experimental data is sufficient for the determination of phase shifts occurring at the diffracting edge and the coupling coefficients for the surface plasmon modes. This analysis will be given in a coming paper.[24]

To conclude, our findings demonstrate that photoemission microscopy is a sensitive, powerful, and versatile tool for the exploration of near-field optical phenomena. We showed that vacuum modes, guided photonic modes, and plasmonic surface modes can directly be visualized in conceptually simple interference experiments. The high spatial resolution of PEEM provided by aberration-corrected electron optics[12,25] allows for quantitative experimentation. Important optical parameters can directly be determined from the obtained images. Details of the optical and plasmonic near-field in nanostructures and metamaterials can be visualized and compared with physical model predictions.

The experimental identification of a photonic vacuum mode above a solid surface, shown in Figure 3, indicates that PEEM can also be used to probe electric fields outside the electron emitting material. The three examples discussed here indicate that a complete visualization of diffraction phenomena including plasmonic and photonic modes and their inter-conversion may be achievable.[20]

The authors gratefully acknowledge funding of this research by the US-DOE Basic Science Office under Contract DE-FG02-10ER46406.

[1]S. Tascu, P. Moretti, S. Kostritskii, and B. Jacquier, Opt. Mater. **24**, 297 (2003).
[2]M. Abashin, P. Tortora, I. Marki, U. Levy, W. Nakagawa, L. Vaccaro, H. Herzig, and Y. Fainman, Opt. Express **14**, 1643 (2006).
[3]A. Kubo, N. Pontius, and H. Petek, Nano Lett. **7**, 470 (2007).
[4]M. Aeschlimann, T. Brixner, A. Fischer, C. Kramer, P. Melchior, W. Pfeiffer, C. Schneider, C. Strüber, P. Tuchscherer, and D. V. Voronine, Science **333**, 1723 (2011).
[5]M. Bauer, D. Bayer, C. Wiemann, and M. Aeschlimann, in *Nonlinear Dynamics of Nanosystems*, edited by G. Radons, B. Rumpf, and H. G. Schuster (WILEY-VCH, Weinheim, 2010), p. 407.
[6]N. M. Buckanie, P. Kirschbaum, S. Sindermann, and F. J. Meyer zu Heringdorf, "Interaction of light and surface plasmon polaritons in Ag Islands studied by nonlinear photoemission microscopy," Ultramicroscopy (published online).
[7]S. J. Peppernick, A. G. Joly, K. M. Beck, and W. P. Hess, J. Chem. Phys. **138**, 154701 (2013).
[8]M. Cinchetti, A. Gloskovskii, S. A. Nepjiko, G. Schönhense, H. Rochholz, and M. Kreiter, Phys. Rev. Lett. **95**, 047601 (2005).
[9]G. H. Fecher, O. Schmidt, Y. Hwu, and G. Schönhense, J. Electron Spectrosc. Relat. Phenom. **126**, 77 (2002).
[10]F. Schertz, M. Schmelzeisen, M. Kreiter, H. J. Elmers, and G. Schönhense, Phys. Rev. Lett. **108**, 237602 (2012).
[11]H. Chen, J. Boneberg, and P. Leiderer, Phys. Rev. B **47**, 9956 (1993).
[12]R. Könenkamp, R. C. Word, G. F. Rempfer, T. Dixon, L. Almaraz, and T. Jones, Ultramicroscopy **110**, 899 (2010).
[13]Z. Guoa, Y. Zhang, Y. D. Mu, L. Xu, S. Xie, and N. Gua, Colloids Surf., A **278**, 33 (2006).
[14]J. Huang, V. Callegari, P. Geisler, C. Brüning, J. Kern, J. C. Prangsma, X. Wu, T. Feichtner, J. Ziegler, P. Weinmann, M. Kamp, A. Forchel, P. Biagioni, U. Sennhauser, and B. Hecht, Nature Commun. **1**, 150 (2010).
[15]J. P. S. Fitzgerald, R. C. Word, S. D. Saliba, and R. Könenkamp, Phys. Rev. B **87**, 205419 (2013).
[16]A. Yariv, *Optical Electronics* (Saunders College Publishing, Philadelphia, 1991).
[17]F. Jenkins and H. White, *Fundamentals of Optics* (McGraw-Hill, New York, 2001).
[18]D. Rosenblatt, A. Sharon, and A. Friesem, IEEE J. Quantum. Electron. **33**, 2038 (1997).
[19]D. Davazoglou, Thin Solid Films **302**, 204 (1997).
[20]P. Lalanne, J. P. Hugonin, H. T. Liu, and B. Wang, Surf. Sci. Rep. **64**, 453 (2009).
[21]P. B. Johnson and R. W. Christy, Phys. Rev. B **6**, 4370 (1972).
[22]E. D. Palik, *Handbook of Optical Constants of Solids* (Academic Press, New York, 1985).
[23]P. Berini, Adv. Opt. Photon. **1**, 484 (2009).
[24]R. C. Word, J. P. S. Fitzgerald, and R. Könenkamp, "Surface plasmon excitation in thin gold films on indium-tin-oxide" (unpublished).
[25]J. P. S. Fitzgerald, R. C. Word, and R. Könenkamp, Ultramicroscopy **115**, 35 (2012).